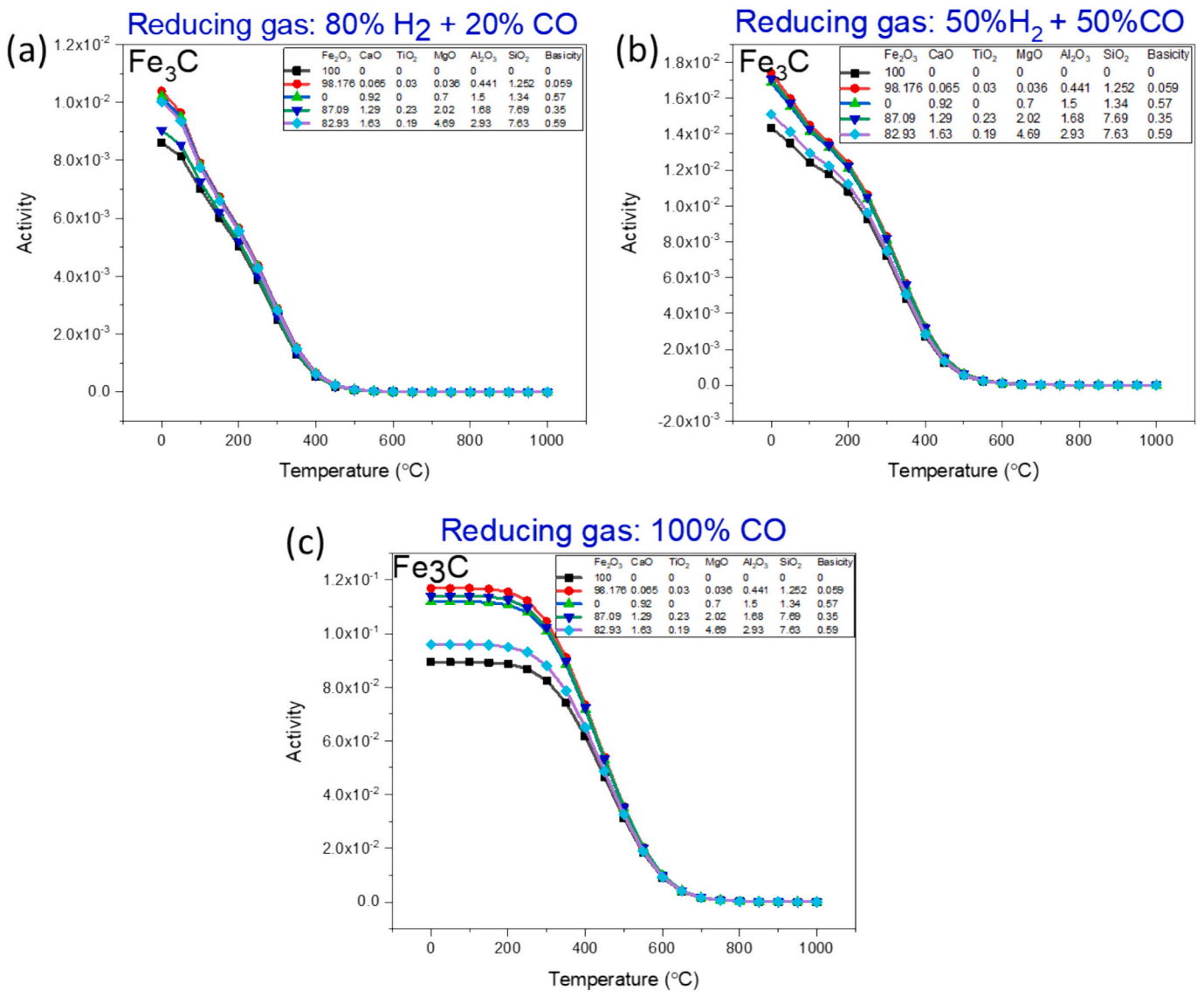

Fig. 11. The effect of oxidic impurity on the evolution of Fe_3C activity (a) 80%H_2 + 20CO, (b) 50%H_2 + 50%CO, (c) 100% CO.

pellet. This non-uniform distribution can lead to local reactions that further reduce the efficiency of the reduction process [47]. In addition, higher tortuosity at higher temperatures leads to a reduction in the reduction rate. This is because the increased complexity of the gas pathways causes turbulence in the pores, which reduces the effective contact between the reducing gasses and the iron oxides. The reduction process becomes less efficient as the gas flow encounters higher resistance, resulting in higher energy consumption and entropy generation. Furthermore, the relationship between tortuosity, entropy generation and energy consumption is particularly pronounced at higher temperatures. Higher tortuosity leads to higher entropy generation due to the more chaotic and restricted gas flow, so that a higher energy input is required to achieve an effective reduction [48]. This non-linear increase in entropy, which is particularly evident in the final stages of reduction, illustrates the thermodynamic challenges that high tortuosity poses. Crucially, the effect of tortuosity is also influenced by the type of reducing gas used [23]. Hydrogen, which is effective at lower temperatures, generally leads to a reduction in tortuosity due to more efficient reduction and less structural deformation of the pellets. In contrast, the use of CO, which requires higher temperatures for effective reduction, can lead to an increase in tortuosity due to greater structural changes within the pellet matrix.

It can also be suggested that when the SiO_2 content is increased to 5%, the formation of the Fe2SiO4 phase significantly hinders the CO reduction of FeO compacts [9]. Conversely, a significantly higher degree of reduction was achieved when the proportion of H_2 in the reducing gas was increased. From a thermodynamic point of view, the direct reduction process with CO gas starts with chemical reactions at the interface and later involves a combination of chemical reactions and gas transport. Reduction with H_2 follows a similar pattern, but oxygen diffusion in the solid state through both the surface and internal structure of the fayalite phase (Fe2SiO4) [49,50] enhances it compared to CO reduction based on oxygen diffusion at the surface. In the presence of 100% H_2 as reducing gas, increasing the temperature up to 950 °C had a more pronounced effect on the activity of the reduced pure iron and the reduction rate when only a small amount of SiO_2 was present [51]. The lower reduction rates and lower activity observed at higher temperatures were related to the formation of a dense iron layer, which hinders contact between FeO and the reducing gas and causes stagnation of the reduction. It can be concluded that by increasing the SiO_2 content, the indirect correlation of activity and reduction rate of pure iron is much more pronounced in an H_2-rich reducing atmosphere.

From a thermodynamic point of view, γ-Al_2O_3 is stable on the nanoscale at a higher temperature of 450 oC and in turn generates local

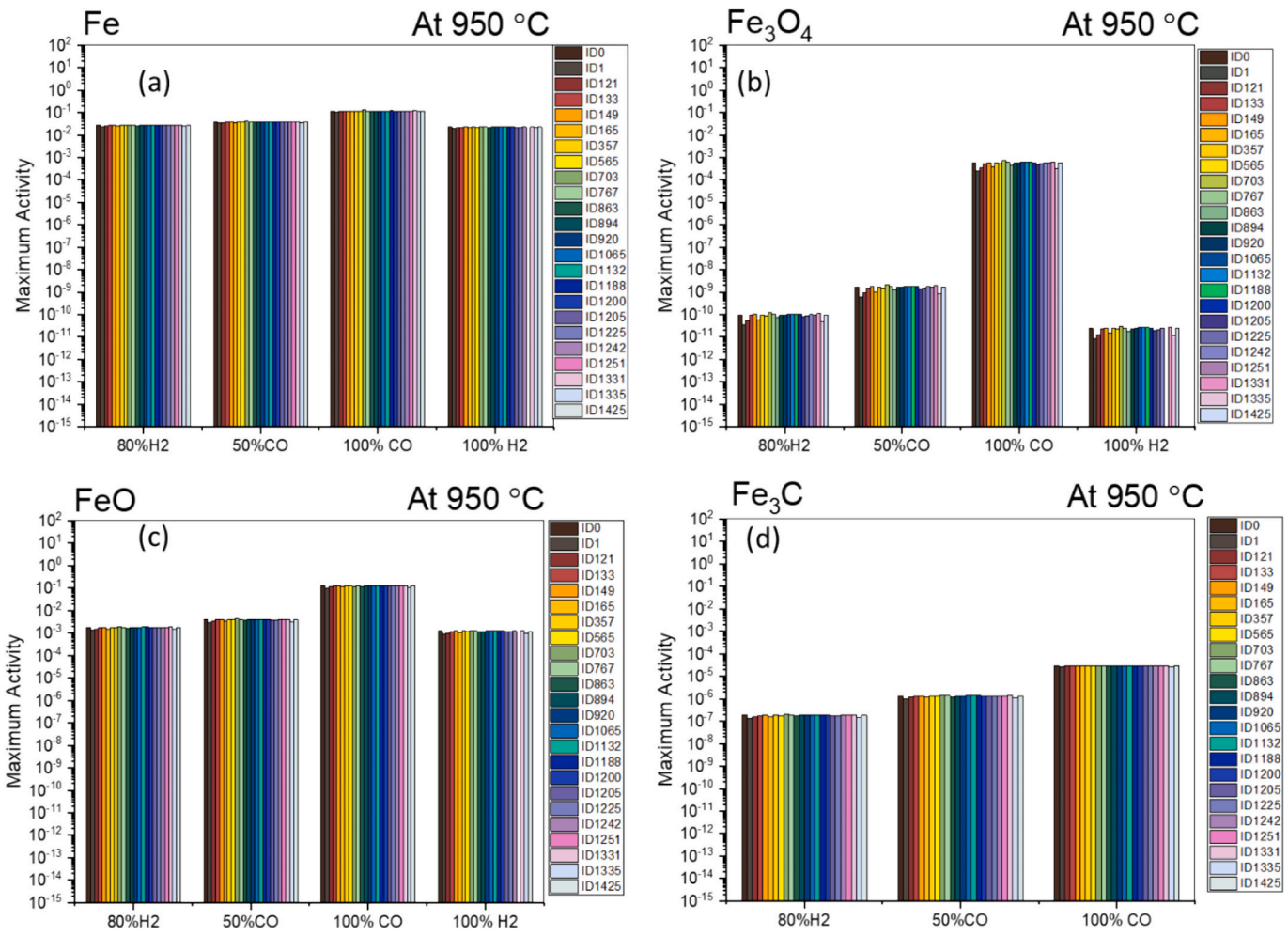

Fig. 12. Average maximum activity in different reducing gas at 950 °C, (a) Fe, (b) Fe_3O_4, (c) FeO, (d) Fe_3C.

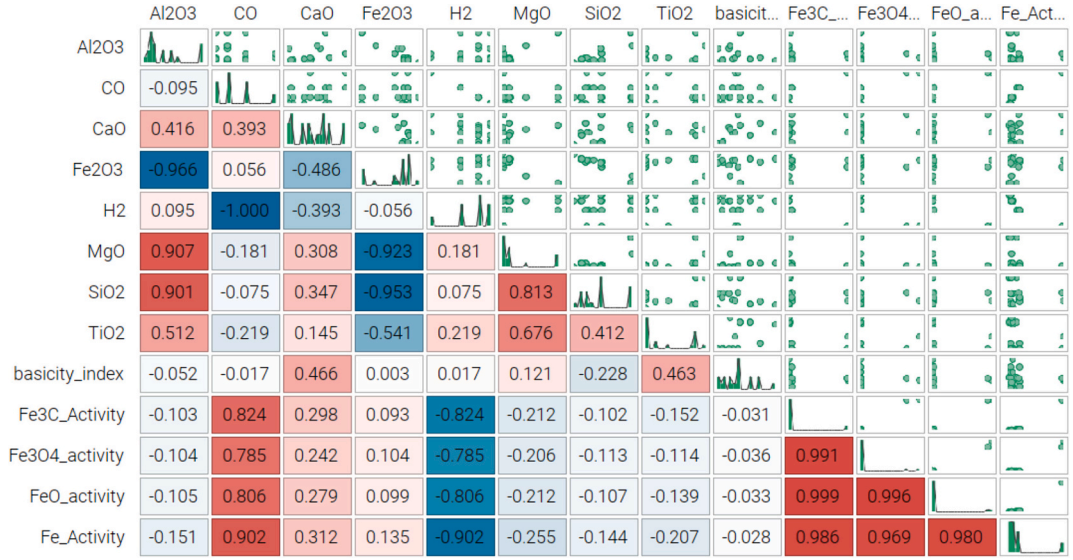

Fig. 13. Scatter matrix for the calculation of activity of iron compounds for all the experienced processing conditions.

stresses, which subsequently cause the formation of micropores and thus inhibit reduction. On the other hand, this can be explained by the inhibition of pore size growth and the formation of surface cracks due to the differences in shrinkage between the dissolved γ-Al_2O_3 and the compact matrix, which increases the number of micropores at the near-surface sites [52]. The formation of surface cracks promotes the reduction rate by facilitating the diffusion of reducing gas [53]. It is reported that in the presence of H_2 as a reducing gas, the addition of 0.5% Al_2O_3

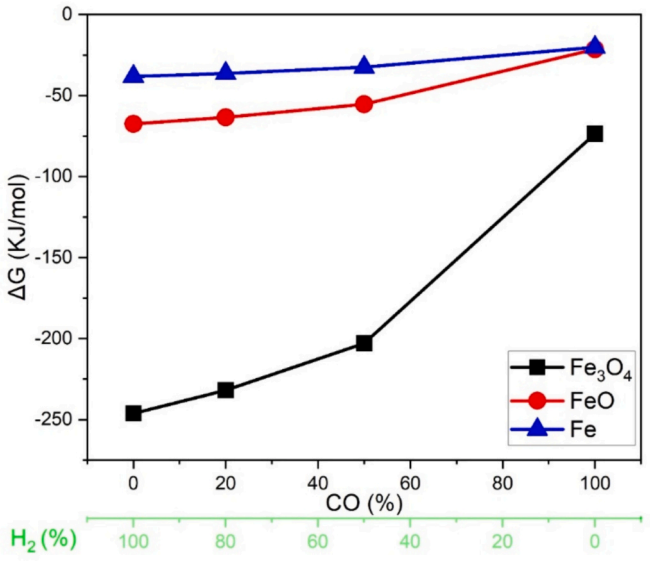

Fig. 14. Gibbs free energy of the reduction of 100% pure pellet of iron oxide to the *Fe_3O_4*, FeO, and Fe at the temperature of 950 °C.

promoted the development of a dense iron layer on the FeO surface, which decreased the reduction rate and the activity of reduced pure iron [54]. Nevertheless, the formation of an iron layer on FeO is much more pronounced by increasing the concentration of dissolved CaO compared to the concentration of dissolved Al_2O_3. Shigematsu et al. [54] reported that this iron layer on FeO is porous, which in turn provides a more active surface for reduction reactions. Further increasing the Al_2O_3 content to 1% led to the formation of hercynite (FeO-Al_2O_3) precipitates, which resulted in an increased reduction rate and consequently led to a lower activity of the iron compounds.

In general, CaO has a positive effect of a maximum of 2 wt% on the direct reduction process [55]. The introduction of CaO into the system leads to a significantly accelerated reduction of FeO compared to pure iron oxide under H_2-rich reduction conditions. This enhanced reduction can be largely attributed to the formation of calcium ferrite, an important reaction pathway as observed in previous studies [45]. However, it is important to note that although increasing the reduction temperature promotes the formation of calcium ferrite, it does not lead to increased reducibility uniformly at all temperature levels. This indicates that the process is influenced by complex interactions and factors beyond temperature. The presence of CaO destabilizes FeO and leads to its decomposition, as can be seen in the following reaction:

$$CaO + 3FeO \rightarrow Fe + 2CaO.Fe_2O_3 \quad (13)$$

The transformation of FeO shows different behaviors depending on whether it consists of pure iron oxide or contains lime additives. In the case of pure iron oxide, the reduction process is primarily influenced by either the diffusion of H_2 through the briquette or the diffusion of Fe through FeO. These diffusion-controlled mechanisms dictate the overall rate of FeO reduction. If, on the other hand, lime is introduced as an additive to iron oxide, a different scenario arises. In this case, the decomposition of FeO, as described in Eq. (14), proves to be the central and rate-controlling step in the reduction process. Unlike in the first scenario, this reaction does not rely on the diffusion of H_2 to accelerate the reduction process. Consequently, the addition of lime leads to a faster reduction of FeO as no H_2 diffusion is required.

$$2CaO.Fe_2O_3 + 3H_2 \rightarrow 2CaO + 2Fe + 3H_2O \quad (14)$$

The effects of the inclusion of CaO in the FeO reduction process are remarkable. At a temperature of 700 °C, the addition of CaO leads to the formation of a dense iron layer covering the FeO grains. Although this dense layer promotes the reduction, it also acts as a barrier and hinders the diffusion of the reducing gas, especially in the CO atmosphere. However, at higher temperatures, which exceed around 700 °C, a different phenomenon occurs. The higher temperature favors the formation of a porous iron structure. In samples containing CaO, this porous iron structure develops on the FeO surface and provides pathways through which the reducing gas can easily diffuse. This effect can be observed over a wide temperature range, up to 100 °C. The beneficial influence of CaO on the reduction process is clearly demonstrated by this porous structure near the reaction interface. However, this positive effect tends to decrease with increasing temperature. This reduction in the positive effect of CaO is primarily due to the decreasing number of pores as the temperature increases. In summary, the accelerated FeO

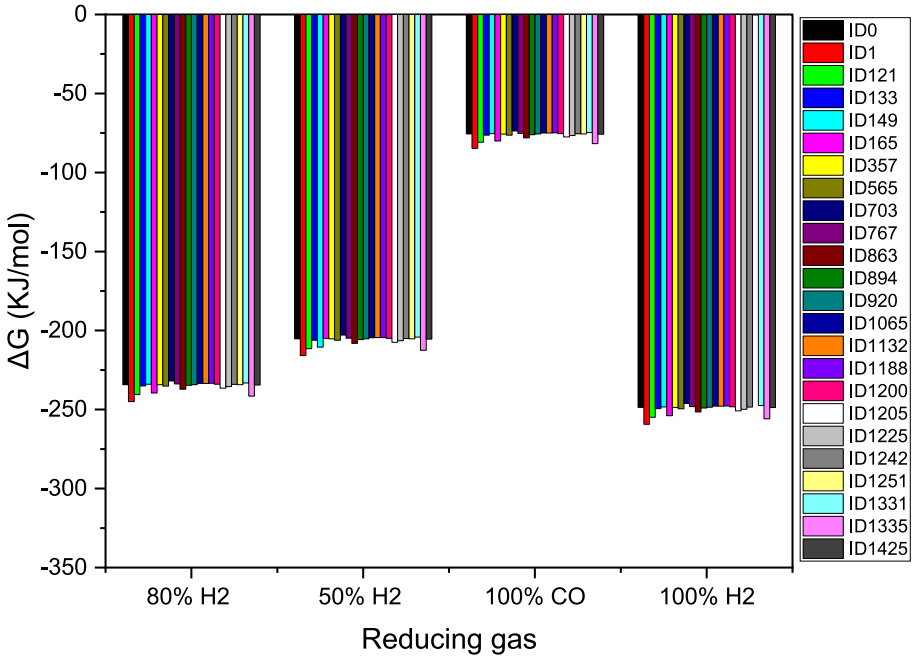

Fig. 15. The Gibbs free energy in different reducing gas at 950 °C, (a) Fe, (b) *Fe_3O_4*, (c) FeO, (d) *Fe_3C*.

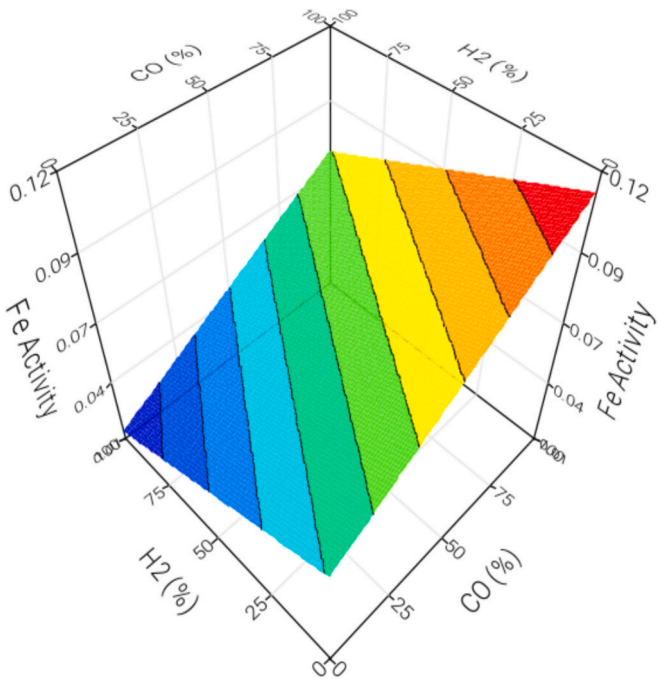

Fig. 16. Fe activity as a function of CO and H_2 percentage in the reducing gas.

reduction favored by CaO can be attributed to the porous nature of the reduced iron near the reaction interface, as already found in previous studies [56].

It is assumed that the presence of Ca ions at the interface between Fe and FeO is the main reason for this phenomenon. It leads to several significant changes: First, the presence of Ca ions at the Fe/FeO interface leads to a decrease in the interfacial energy between these materials [57]. This reduction in energy favors the disintegration of the iron layer, making it easier to degrade. Secondly, the introduction of Ca ions at this interface enhances the adsorption of other calcium ions [58], which further influences the surface interactions and supports the disintegration of the iron layer. This increased adsorption of calcium ions serves to enhance the effects of CaO on the reduction process. Finally, the energy of interfacial deformation or the mismatch of lattice parameter between iron and iron oxide is altered by the presence of Ca ions. This change in the lattice parameter of the oxide and the resulting changes in strain energy contribute to the overall collapse of the iron layer as they lead to changes in the structural integrity of the interface [59].

The presence of 1 mol% MgO had the greatest effect on promoting the activity and reduction of FeO defiance, increasing the MgO content to 5 mol% showed a negligible effect, which was attributed to the differences in iron morphology formed during reduction [60,61]. In agreement with previous studies [62], it can be concluded that Mg_2^+ could diffuse into the Fe_3O_4 lattice and form a $MgFe_2O_4$ solid solution by replacing part of the $Fe2^+$, making the structure porous. The higher porosity improved the diffusion of the reducing gas and increased the contact areas, promoting the reduction process. On the other hand, the gas diffusion becomes more turbulent as the tortuosity of the pores increases, leading to a decrease in the reduction rate with increasing tortuosity [23,48]. The introduction of MgO into Fe_3O_4 appears to play a crucial role in promoting the formation of magnesiospinels, a development that effectively promotes the formation of a porous structure within the material [60]. This porous structure helps to create pathways for various reactions and the exchange of gasses, resulting in enhanced porosity and reactivity. Conversely, in the presence of MgO, FeO shows a marked transformation leading to denser structures. This transformation can be attributed to the formation of magnesiowustite, which, in contrast to the porous nature of magnesiospinels, contributes to a more compact and solid composition. This structural change can significantly affect the properties and behavior of the material. However, it is important to note that the addition of 0.5 wt% MgO to the charged iron ore in the final stage of reduction had a hindering effect, particularly in the transition from FeO to pure Fe. This observation suggests that while MgO is beneficial for certain aspects of the reduction process, it may present challenges or complications at certain stages of the iron ore reduction process, as documented in previous research [63].

The influence of various additives on the reduction behavior of Fe_2O_3 and Fe_3O_4 pellets was investigated in detail, revealing different effects. In particular, the addition of CaO was found to have a suppressive effect on the reduction rate of both Fe_2O_3 and Fe_3O_4 pellets, while SiO_2 showed no significant effect. This particular influence of CaO on the reduction process can be attributed to the formation of molten calcium ferrite, a phase that subsequently obstructs the existing pores within the Fe_2O_3 pellets. Furthermore, it was observed that the estimated effective gas diffusivity decreased significantly when high concentrations of CaO and SiO_2 were introduced into the pellet, suggesting that these additives may hinder gas diffusion pathways within the pellet structure. Furthermore, at high H_2 flow rates, CaO and to a lesser extent MgO were observed to promote the local formation of porous iron nuclei. This phenomenon helps to create pathways for rapid gas diffusion and consequently facilitates the reduction process. However, in contrast to CaO and MgO, samples containing SiO_2 and Al_2O_3 showed no discernible effect on the formation of porous iron nuclei, suggesting that these additives do not have a significant influence on the development of these essential porous structures within the pellet matrix, as documented in

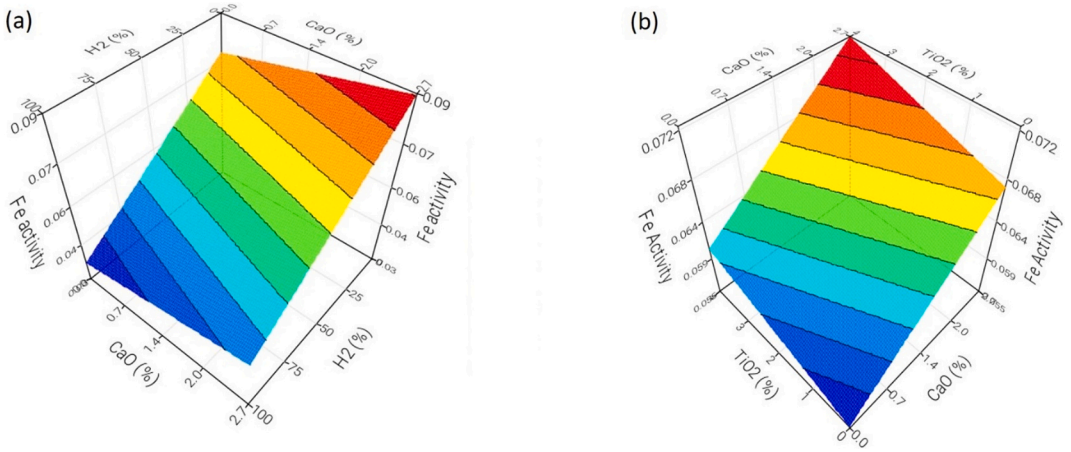

Fig. 18. Fe activity as a function of (a) CaO and H_2 percentage, (b) CaO and TiO_2 in the pellet.

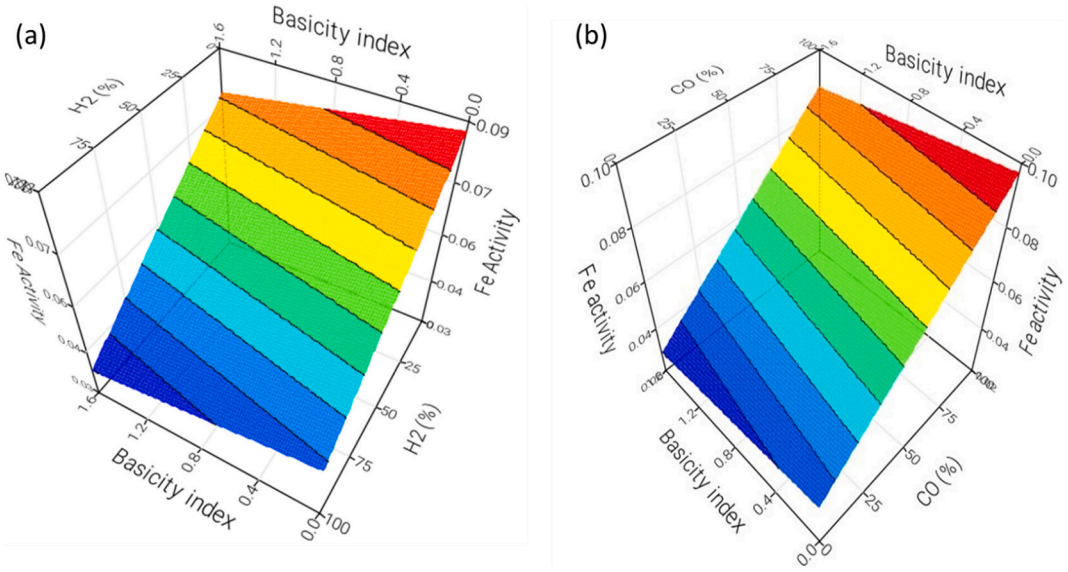

Fig. 17. Fe activity as a function of basicity index and (a) H_2 percentage, (b) CO in the reducing gas.

previous studies [42].

The Fe_3C activity are largely influenced by non-iron oxides such as TiO_2 and CaO with a direct proportionality as shown in Fig. 19.

The effects of non-ferrous oxides on the behavior of Al_3C show the complex interplay between these catalyst components, their synergistic effects and their influence on the catalytic activity. CaO, MgO, TiO_2 and Al_2O_3 are well-known industrial catalysts, and their influence on the activity of Fe_3C can be attributed to their ability to change the surface properties, chemical reactivity and electronic structure of the catalysts. For example, CaO and MgO are basic oxides and can serve as strong bases that can influence the acidity of the catalytic sites on the Al3C surface, affecting the adsorption and activation of reaction molecules. In addition, the interaction between TiO_2 and Al_2O_3 with Al_3C in the presence of H_2 gas as a reducing agent shows a particularly intriguing trend. This suggests that the interplay between multiple oxide additions can lead to synergistic effects or improved catalytic performance. For example, it has been found in the literature that the presence of Al_2O_3 can promote the dispersion and stability of TiO_2 on the catalyst surface, which in turn can improve the redox properties and thus the catalytic activity of Al3C [64]. Moreover, the cooperation between CaO and MgO in the presence of H_2 gas seems to emphasize the importance of considering multiple oxide components in the development of catalysts for certain reactions. The presence of MgO can promote the accessibility of active sites on the Al3C surface and increase reactivity towards certain reactants when used together with CaO.

The original iron ore was characterized by a remarkably homogeneous distribution of various common nanoscale impurities, including sodium (Na), magnesium (Mg), aluminum (Al), titanium (Ti) and vanadium (V). However, during the reduction process, the resulting samples showed a distinct change, namely the formation of nano-sized oxide islands embedded in the reduced iron matrix. These oxide islands consist of species derived from the non-ferrous oxides that were present in the original composition of the ore. Since these oxide species could not be effectively reduced during the process, they faced a crucial choice: they could either maintain their original uniform distribution as oxide nanoparticles or be displaced from the reduction front and eventually become part of the remaining oxide phase. This phenomenon points to a compelling mechanism at play in the reduction of iron ore. The driving force behind the reduction of iron was apparently strong enough to overcome this particular barrier and eventually entrap the gangue oxides as nanoparticles in the iron matrix [65]. This process demonstrates the intriguing interplay between the reduction forces and the persistence of non-iron oxide species within the transformed material, as described in previous research [66].

The reduction process exhibits different mechanisms in different phases, in particular gas diffusion and chemical reactions at the interfaces. The behavior varies depending on the atmosphere of the reducing gas. In particular, H_2 shows faster reduction kinetics compared

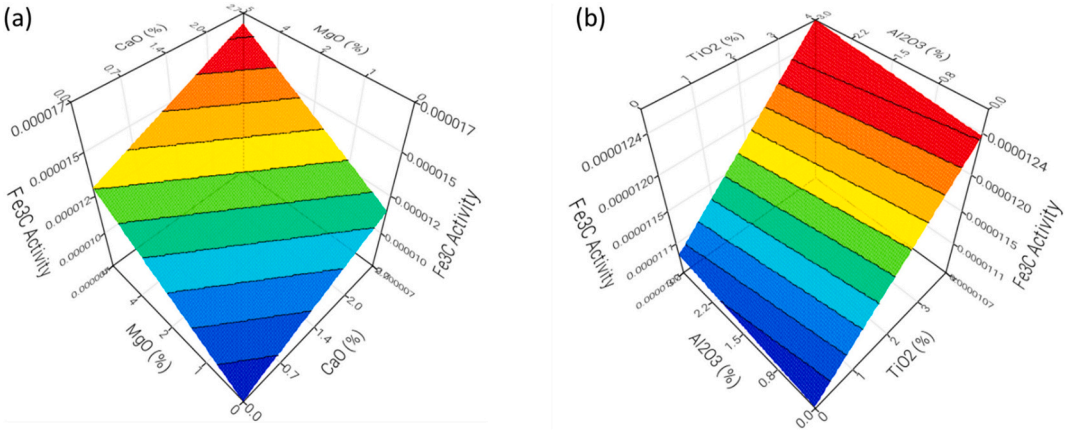

Fig. 19. Fe_3C activity as a function of (a) CaO and MgO percentage, (b) TiO_2 and Al_2O_3 in the pellet.

to CO. During the reduction of Fe_2O_3 pellets in an H_2 atmosphere, the first two reduction stages, from Fe_2O_3 to Fe_3O_4 and from Fe_3O_4 to FeO, take place quickly, while the reduction of FeO to pure iron is slow. This discrepancy is due in part to the unique physical properties of H_2, including its smaller molecular size and lower viscosity, which can lead to different gas transport phenomena compared to carbon-based reducing agents. The effect of these non-ferrous oxides is more pronounced at lower temperatures and is enhanced at larger pellet sizes. Regardless of the specific non-ferrous oxide, the overall process exhibits common trends, including mass loss due to oxygen removal, increased porosity and volume expansion, especially for samples processed at temperatures above 1000 °C. These high-temperature conditions can lead to cracks in the reduced pellets, reducing their mechanical strength and potentially generating fines and dust that impair gas permeability in the shaft furnace. The formation of cracks is attributed to the restructuring of the crystal lattice during phase transformations, resulting in stresses and lattice disruptions. In the presence of several impurities and non-ferrous oxides, several factors contribute to fluctuations in the reduction process. For example, the presence of CaO leads to the formation of calcium ferrite, which increases the reduction rate. However, this effect decreases at higher temperatures due to changes in the pore structure. In addition, the introduction of MgO can either promote or hinder the reduction, depending on its concentration and its effect on the porosity of the pellets.

Previous studies by various researchers looking at the reduction of iron ore have consistently emphasized the negative Gibbs free energy associated with the reduction processes leading to Fe_3O_4, FeO and Fe. This negativity indicates the spontaneity of the reaction, with temperature and the nature of the reducing gas influencing the dynamics of the Gibbs free energy [10,29,67]. In the work of Tahari et al. [29], it was observed that at 500 °C the thermodynamic preference of reduction by CO over H_2 is evident. In particular, the formation of Fe_3O_4 in a CO atmosphere is more favorable compared to H_2 at this temperature. The reported Gibbs free energy values for the reduction of Fe_2O_3 to Fe_3O_4 at 500 °C were − 83 and − 75 kJ/mol in CO and H_2 atmospheres, respectively, emphasizing the greater spontaneity of Fe_3O_4 formation under CO reductant. In addition, an increase in temperature increases the negative Gibbs free energy, which is consistent with similar findings from another research [68]. The temperature-dependent trend is consistent: higher temperatures lead to a more negative Gibbs free energy for Fe_3O_4 production in both CO and H_2 atmospheres. This pattern is reflected in our studies, as shown in Figs. 13 and 14, where Fe_3O_4 formation proves to be the most spontaneous compared to FeO and Fe. It is noteworthy that at higher temperatures (950 °C) an H_2 atmosphere seems to increase the efficiency of the reduction process compared to CO. In summary, the collective presence of several non-ferrous oxides such as SiO_2, Al_2O_3, CaO, TiO_2 and MgO significantly affects the direct reduction of iron oxide pellets, regardless of whether CO gas or H_2 is used as a reducing agent. These non-iron oxides influence the reduction process through their interaction. For example, the formation of different phases, such as calcium ferrite or magnesioFeO, can influence the overall porosity of the pellets. This in turn affects the diffusion of the reducing gasses and the contact surfaces within the pellet and ultimately influences the reduction rate. In addition, all these factors together can influence the effective gas diffusivity within the pellet, which affects the mass transfer of the reducing gasses and the chemical reactions at the interfaces. This collective influence can lead to variations in the reduction kinetics at different temperatures and gas compositions. These impurities, which often remain in the pellets during DR processes, lead to a high slag load in the subsequent EAF operations, which makes it necessary to use high-quality pellets with an impurity level of <5%.

4. Conclusion

In summary, this study provides a comprehensive investigation of the reduction of iron oxide pellets and provides valuable insight into the effects of different reducing gas atmospheres and impurities on the equilibrium amounts and activity of iron compounds using HSC chemistry software. The conclusions can be drawn as follows:

- The study confirms that H_2 as a reducing gas promotes more effective reduction of iron oxide pellets at lower temperatures, resulting in higher equilibrium levels of Fe. Conversely, CO proves to be more effective at higher temperatures, indicating an atmospheric dependence on temperature for optimal reduction performance. This result highlights the importance of selecting appropriate gas atmospheres based on operating temperature ranges to maximize reduction behavior.
- The structural effects of the reducing gasses were notable, with hydrogen reducing the tortuosity of the pellets more effectively at lower temperatures. This is due to its smaller molecular size, which increases diffusion rates. In contrast, CO increases tortuosity, necessitating higher temperatures that cause more pronounced structural changes within the pellets. Understanding these dynamics is crucial for the development of pellet structures that are compatible with certain reducing gasses.
- From a thermodynamic point of view, the reduction reactions of iron oxide are shown to occur spontaneously at 950 °C in different gas atmospheres, with the reduction of Fe_3O_4 exhibiting the lowest Gibbs free energy. CaO and MgO in particular play a crucial role in modulating the reduction kinetics, especially enhancing the reduction of Fe_3O_4 in a hydrogen-rich atmosphere.
- Porosity in iron oxide pellets is the key to efficient reduction and varies with the reducing atmosphere. H_2 promotes early porosity and improves reduction at lower temperatures, while CO requires higher temperatures to be effective and forms less porosity initially. A mixture of 50% H_2 and 50% CO takes advantage of the early benefits of hydrogen and the effectiveness of CO at higher temperatures, optimizing reduction behavior in iron and steel production.
- The results show that impurities such as TiO_2, CaO, SiO_2, MgO and Al_2O_3 significantly influence the reduction activity of iron and its oxides. In particular, CaO and MgO play a crucial role in modulating the reduction kinetics and especially promote the reduction of Fe_3O_4 in a hydrogen-rich atmosphere.

In summation, the findings presented in this paper advance our understanding of the direct reduction process and highlight the multifaceted interplay of factors involved. Such knowledge is indispensable for optimizing reduction processes in the iron and steel industry, leading to more efficient and sustainable operations. This study paves the way for further research and practical applications in this critical sector of industrial production.

CRediT authorship contribution statement

Behzad Sadeghi: Writing – review & editing, Writing – original draft, Visualization, Validation, Project administration, Methodology, Investigation, Data curation, Conceptualization. **Mojtaba Najafizadeh:** Writing – original draft, Software, Formal analysis. **Pasquale Cavaliere:** Writing – review & editing, Validation, Supervision, Software, Resources, Methodology, Investigation, Funding acquisition. **Ali Shabani:** Writing – review & editing, Validation, Conceptualization. **Marieh Aminaei:** Writing – review & editing, Software, Data curation.

Declaration of competing interest

None.

Data availability

Data will be made available on request.

Acknowledgments

The authors would like to thank the Italian Ministry for University and Research (MUR) for the fundings provided under the Grant" green H_2 for clean steels, kinetics and modeling in the direct reduction of iron oxides, decarbonization of hard to abate industry– "real-green-steels", P202278BNF.

References

[1] W. Yan-kun, Application of HSC chemistry software in university chemical scientific research, J. Henan Inst. Educ. 2 (2013) 32–34.
[2] A. Roine, HSC - Software Ver. 3.0 for Thermodynamic Calculations, 1989.
[3] A. Zare Ghadi, M.S. Valipour, S.M. Vahedi, H.Y. Sohn, A review on the modeling of gaseous reduction of iron oxide pellets, Steel Res. Int. 91 (2020) 1900270.
[4] M.K. Goenka, A. Naik, Effect of Size Distribution and Water Content on Properties of Iron Ore Pellets, 2013.
[5] P. Metolina, T.R. Ribeiro, R. Guardani, Hydrogen-based direct reduction of industrial iron ore pellets: statistically designed experiments and computational simulation, Int. J. Miner. Metall. Mater. 29 (2022) 1908–1921.
[6] P. Cavaliere, L. Dijon, A. Laska, D. Koszelow, Hydrogen direct reduction and reoxidation behaviour of high-grade pellets, Int. J. Hydrog. Energy 49 (2023) 1235–1254.
[7] M. Kazemi, M.S. Pour, D. Sichen, Experimental and modeling study on reduction of Fe_2O_3 pellets by hydrogen gas, Metall. Mater. Trans. B Process Metall. Mater. Process. Sci. 48 (2017) 1114–1122.
[8] W.R. Morrow, A. Hasanbeigi, J. Sathaye, T. Xu, Assessment of energy efficiency improvement and CO2 emission reduction potentials in India's cement and iron & steel industries, J. Clean. Prod. 65 (2014) 131–141.
[9] R. An, B. Yu, R. Li, Y.-M. Wei, Potential of energy savings and CO2 emission reduction in China's iron and steel industry, Appl. Energy 226 (2018) 862–880.
[10] K. Jabbour, N. El Hassan, Optimized conditions for reduction of iron (III) oxide into metallic form under hydrogen atmosphere: a thermodynamic approach, Chem. Eng. Sci. 252 (2022) 117297.
[11] V. Vogl, M. Åhman, What Is Green Steel?: Towards a Strategic Decision Tool for Decarbonising EU Steel, 2019.
[12] B. Gamisch, L. Huber, M. Gaderer, B. Dawoud, On the kinetic mechanisms of the reduction and oxidation reactions of Iron oxide/Iron pellets for a hydrogen storage process, Energies 15 (2022) 8322.
[13] I.R. Souza Filho, H. Springer, Y. Ma, A. Mahajan, C.C. da Silva, M. Kulse, D. Raabe, Green steel at its crossroads: hybrid hydrogen-based reduction of iron ores, J. Clean. Prod. 340 (2022) 130805.
[14] Y. Ma, I.R. Souza Filho, Y. Bai, J. Schenk, F. Patisson, A. Beck, J.A. van Bokhoven, M.G. Willinger, K. Li, D. Xie, D. Ponge, S. Zaefferer, B. Gault, J.R. Mianroodi, D. Raabe, Hierarchical nature of hydrogen-based direct reduction of iron oxides, Scr. Mater. 213 (2022) 114571.
[15] P. Cavaliere, A. Perrone, D. Marsano, V. Primavera, Hydrogen-Based Direct Reduction of Iron Oxides Pellets Modeling, Steel Research International, 2023, p. 2200791.
[16] S. Li, H. Gu, A. Huang, Y. Zou, S. Yang, L. Fu, Thermodynamic analysis and experimental verification of the direct reduction of iron ores with hydrogen at elevated temperature, J. Mater. Sci. 57 (2022) 20419–20434.
[17] S. Pauliuk, R.L. Milford, D.B. Muller, J.M. Allwood, The steel scrap age, Environ. Sci. Technol. 47 (2013) 3448–3454.
[18] Q. Fradet, M. Kurnatowska, U. Riedel, Thermochemical reduction of iron oxide powders with hydrogen: review of selected thermal analysis studies, Thermochim. Acta 726 (2023) 179552.
[19] M. Sastri, R. Viswanath, B. Viswanathan, Studies on the reduction of iron oxide with hydrogen, Int. J. Hydrog. Energy 7 (1982) 951–955.
[20] M. Lara, J. Camporredondo, A. Garcia, L. Castruita, F. Equihua, H. Moreno, M. Corona, Thermodynamic simulation of reduction of mixtures of iron ore, siderurgical wastes and coal, Metalurgija 58 (2019) 11–14.
[21] W.-H. Chen, C.-L. Hsu, S.-W. Du, Thermodynamic analysis of the partial oxidation of coke oven gas for indirect reduction of iron oxides in a blast furnace, Energy 86 (2015) 758–771.
[22] W.-H. Chen, M.-R. Lin, T.-S. Leu, S.-W. Du, An evaluation of hydrogen production from the perspective of using blast furnace gas and coke oven gas as feedstocks, Int. J. Hydrog. Energy 36 (2011) 11727–11737.
[23] P. Cavaliere, A. Perrone, D. Marsano, Effect of reducing atmosphere on the direct reduction of iron oxides pellets, Powder Technol. 426 (2023) 118650.
[24] L.-Y. Yi, Z.-C. Huang, H. Peng, T. Jiang, Action rules of H_2 and CO in gas-based direct reduction of iron ore pellets, J. Cent. South Univ. 19 (2012) 2291–2296.
[25] X. Mao, P. Garg, X. Hu, Y. Li, S. Nag, S. Kundu, J. Zhang, Kinetic analysis of iron ore powder reaction with hydrogen—CO, Int. J. Miner. Metall. Mater. 29 (2022) 1882–1890.
[26] P. Ebrahimi, A. Kumar, M. Khraisheh, A review of recent advances in water-gas shift catalysis for hydrogen production, Emerg. Mater. 3 (2020) 881–917.
[27] W.K. Jozwiak, E. Kaczmarek, T.P. Maniecki, W. Ignaczak, W. Maniukiewicz, Reduction behavior of iron oxides in hydrogen and CO atmospheres, Appl. Catal. A Gen. 326 (2007) 17–27.
[28] D. Spreitzer, J. Schenk, Reduction of iron oxides with hydrogen—a review, Steel Res. Intern. 90 (2019) 1900108.
[29] M. Tahari, F. Salleh, T.S.T. Saharuddin, N. Dzakaria, A. Samsuri, M. Hisham, M. A. Yarmo, Influence of hydrogen and various CO concentrations on reduction behavior of iron oxide at low temperature, Int. J. Hydrog. Energy 44 (2019) 20751–20759.
[30] W.F. Jiang, J.-Y. Hwang, S.J. Hao, Y.Z. Zhang, Effect of Carbon Coating on Fe_3O_4 Reduction, 2018.
[31] W.-H. Chen, M.-R. Lin, A. Yu, S.-W. Du, T.-S. Leu, Hydrogen production from steam reforming of coke oven gas and its utility for indirect reduction of iron oxides in blast furnace, Int. J. Hydrog. Energy 37 (2012) 11748–11758.
[32] H. Ho-Sun, C. Uoo-Chang, C. Won-Sub, C. Won-Bae, Characteristics of Carbidization for Iron ore fines with a wide size range, J. Korean Inst. Resources Recycl. 12 (2003) 42–49.
[33] E.M. Cohn, E.H. Bean, M. Mentser, L.J.E. Hofer, A.P. Pontello, W.C. Peebles, K. H. Jack, The carburization of iron oxide with CO: modifications of hägg Fe_3C, J. Chem. Technol. Biotechnol. 5 (2007) 418–425.
[34] W. De, Kinetics Behavior of Producing Fe_3C in Fluidized Bed, Journal of Northeastern University, 2002.
[35] A. Zakeri, K.S. Coley, L. Tafaghodi, Hydrogen-based direct reduction of Iron oxides: a review on the influence of impurities, Sustainability 15 (2023) 13047.
[36] Y. Ma, I.R.S. Filho, X. Zhang, S. Nandy, P. Barriobero-Vila, G. Requena, D. Vogel, M. Rohwerder, D. Ponge, H. Springer, D. Raabe, Hydrogen-based direct reduction of iron oxide at 700°C: heterogeneity at pellet and microstructure scales, Int. J. Miner. Metall. Mater. 29 (2022) 1901.
[37] R.K. Dishwar, O.P. Sinha, Effect of basicity on the activation energy during reduction of highly fluxed iron ore pellets, Fuel 296 (2021) 120640.
[38] A.F.H. Wielers, A.J.H.M. Kock, C.E.C.A. Hop, J.W. Geus, A.M. Kraan, The reduction behavior of silica-supported and alumina-supported iron catalysts: a Mössbauer and infrared spectroscopic study, J. Catal. 117 (1989) 1–18.
[39] H.-B. Zuo, C. Wang, J.-J. Dong, K.-X. Jiao, R.-S. Xu, Reduction kinetics of iron oxide pellets with H_2 and CO mixtures, Int. J. Miner. Metall. Mater. 22 (2015) 688–696.
[40] M. Bahgat, M. Khedr, Reduction kinetics, magnetic behavior and morphological changes during reduction of Fe_3O_4 single crystal, Mater. Sci. Eng. B 138 (2007) 251–258.
[41] A. Ranzani da Costa, D. Wagner, F. Patisson, Modelling a new, low CO2 emissions, hydrogen steelmaking process, J. Clean. Prod. 46 (2013) 27–35.
[42] N. Shigematsu, H. Iwai, Effects of initiation of reduction and oxide additives on morphology of Iron nuclei in the reduction of FeO with hydrogen at 670° C, Tetsu-to-hagané 79 (1993) 1032–1038.
[43] T.S. Paananen, K. Kinnunen, Effect of TiO_2-content on reduction of Iron ore agglomerates, Steel Research Intern. 80 (2009).
[44] S. Bonanni, K. Aït-Mansour, W. Harbich, H. Brune, Effect of the TiO_2 reduction state on the catalytic CO oxidation on deposited size-selected Pt clusters, J. Am. Chem. Soc. 134 (7) (2012) 3445–3450.
[45] M. Bahgat, K. Abdel Halim, M. Nasr, A. El-Geassy, Morphological changes accompanying gaseous reduction of SiO_2 doped FeO compacts, Ironmak. Steelmak. 35 (2008) 205–212.
[46] B. Sadeghi, P. Cavaliere, M. Bayat, N. Ebrahimzadeh Esfahani, A. Laska, D. Koszelow, Experimental study and numerical simulation on porosity dependent direct reducibility of high-grade iron oxide pellets in hydrogen, Int. J. Hydrog. Energy 69 (2024) 586–607.
[47] P. Cavaliere, A. Perrone, L. Dijon, A. Laska, D. Koszelow, Direct reduction of pellets through hydrogen: experimental and model behaviour, Int. J. Hydrog. Energy 49 (2023) 1444–1460.
[48] A. Zare Ghadi, M. Valipour, M. Biglari, Transient entropy generation analysis during FeO pellet reduction to sponge iron, Int. J. Eng. 31 (2018) 1274–1282.
[49] K. Ullrich, K.D. Becker, Kinetics and diffusion of defects in fayalite, Fe2SiO4, Solid State Ionics 141 (2001) 307–312.
[50] W.-H. Kim, Y.-S. Lee, I.-K. Suh, D.-J. Min, Influence of CaO and SiO_2 on the reducibility of FeO using H_2 and CO gas, ISIJ Int. 52 (2012) 1463–1471.
[51] N. Shigematsu, H. Iwai, Effect of the addition of SiO_2 and SiO_2-CaO on the reduction of dense FeO at high temperatures, Tetsu-to-Hagané 79 (1993) 920–926.
[52] Y. Suzuki, M. Yamamoto, T. Kotanigawa, K. Nishida, Some aspects on porous properties of iron oxides containing foreign oxides reduced by hydrogen, Metall. Trans. B 12 (1981) 691–697.
[53] K. Higuchi, R.H. Heerema, Influence of artificially induced porosity on strength and reduction behavior of Fe_2O_3 compacts, ISIJ Int. 45 (2005) 574–581.
[54] N. Shigematsu, H. Iwai, Effect of the addition of Al_2O_3 and Al_2O_3-Ca0 on the reduction of dense FeO with H_2, Tetsu-to-Hagané 73 (1987) 2243–2250.
[55] B.L. Seth, H. Ross, The effect of lime on the reducibility of Iron-oxide agglomerates, Can. Metall. Q. 2 (1963) 15–30.
[56] Y. Iguchi, M. Fukunaga, J. Hirao, Dependence of the reduction rate on the temperature and the α-γ transformation in FeO containing CaO, Trans. Jpn. Inst. Metals 24 (1983) 115–124.
[57] A. Matamoros-Veloza, R. Barker, S.M. Vargas, A. Neville, Iron calcium carbonate instability: structural modification of siderite corrosion films, ACS Appl. Mater. Interfaces 12 (2020) 49237–49244.
[58] J. Heo, B.-S. Kim, J.H. Park, Effect of CaO addition on Iron recovery from copper smelting slags by solid carbon, Metall. Mater. Trans. B 44 (2013) 1352–1363.
[59] Z.-L. Zhao, H. Tang, Z. Guo, Effects of CaO on precipitation morphology of metallic Iron in reduction of Iron oxides under CO atmosphere, J. Iron Steel Res. Int. 20 (2013) 16–24.
[60] D.Q. Zhu, J. Chou, B.-J. Shi, J. Pan, Influence of MgO on low temperature reduction and mineralogical changes of sinter in simulated COREX shaft furnace reducing conditions, Minerals 9 (2019) 272.
[61] L.-H. Hsieh, J.A. Whiteman, Effect of raw material composition on the mineral phases in lime-fluxed Iron ore sinter, ISIJ Int. 33 (1993) 462–473.

[62] F. Pan, Q. Zhu, Z. Du, H. Sun, Migration behavior of the MgO and its influence on the reduction of Fe_3O_4–MgO sinter, ISIJ Int. 58 (2018) 652–659.
[63] M. Bahgat, K.S.A. Halim, M.I. Nasr, A.H.A. El-Geassy, Reduction behaviour of FeO doped with MgO, Steel Res. Intern. 78 (2007) 443–450.
[64] W.R. Rao, I.B. Cutler, Effect of Iron oxide on the sintering kinetics of Al_2O_3, J. Am. Ceram. Soc. 56 (1973) 588–593.
[65] C. Gleitzer, Some remarkable features in the reduction of iron oxides, Solid State Ionics 38 (1990) 133–141.
[66] S.-H. Kim, X. Zhang, Y. Ma, I.R. Souza Filho, K. Schweinar, K. Angenendt, D. Vogel, L.T. Stephenson, A.A. El-Zoka, J.R. Mianroodi, M. Rohwerder, B. Gault, D. Raabe, Influence of microstructure and atomic-scale chemistry on the direct reduction of iron ore with hydrogen at 700°C, Acta Mater. 212 (2021) 116933.
[67] X. Zheng, S. Paul, L. Moghimi, Y. Wang, R.A. Vilá, F. Zhang, X. Gao, J. Deng, Y. Jiang, X. Xiao, Correlating chemistry and mass transport in sustainable iron production, Proc. Natl. Acad. Sci. 120 (2023) e2305097120.
[68] Y. Xiao, K. Zhu, S. Ye, Z. Xie, Y. Zhang, X. Lu, Hydrogen on softening-melting and slag forming behavior under the operation of blast furnace with iron coke charging, Int. J. Hydrog. Energy 47 (2022) 31129–31139.